Orthogonality constrained gradient reconstruction for superconvergent linear functionals

Roberto Porcù[2,3], **Maurizio M. Chiaramonte**[1,2]

Received: date / Accepted: date

Abstract The post-processing of the solution of variational problems discretized with Galerkin finite element methods is particularly useful for the computation of quantities of interest. Such quantities are generally expressed as linear functionals of the solution and the error of their approximation is bounded by the error of the solution itself. Several *a posteriori* recovery procedures have been developed over the years to improve the accuracy of post-processed results. Nonetheless such recovery methods usually deteriorate the convergence properties of linear functionals of the solution and, as a consequence, of the quantities of interest as well. The paper develops an enhanced gradient recovery scheme able to both preserve the good qualities of the recovered gradient and increase the accuracy and the convergence rates of linear functionals of the solution.

Keywords superconvergent patch recovery · linear functionals · Barlow points · goal-oriented error estimation · quantities of interest

1 Introduction

In this work, we develop a novel gradient reconstruction technique aimed at increasing the accuracy of the gradient approximant and the linear functionals thereof.

While much effort has been devoted to *a posteriori* gradient reconstruction techniques (*cf.* for example [23]) the goal of most methods is an improved approximation of the gradient without regards for their corresponding linear functionals. As these functionals encode important information which can be useful for many applications, it can be very beneficial computing these functionals with a high order of accuracy.

✉ M. M. Chiaramonte - E-mail: mchiaram@fb.com

[1]Facebook Reality Labs, Redmond, WA 98052

[2]Department of Civil and Environmental Engineering, Princeton University, Princeton, NJ 08540, USA

[3]The Center for Computational Sciences and Engineering, Lawrence Berkeley National Laboratory, Berkeley, CA 94720, USA

The work contained herein is mostly driven by the importance of quantities of interest in engineering analysis. Some examples of quantities of interest for physics applications are averages, flow rates, velocities, temperatures, shear stresses, stress intensity factors in fracture mechanics, to name a few.

In the context of adaptivity, the *a posteriori* evaluation of the error of a given quantity of interest is in general exploited in order to improve the accuracy of that particular quantity, see for example [4,12,16,21,27,31,34,40]. Duality-based approaches to *a posteriori* goal-oriented error estimation are described in [11,17,18, 33]. Specific techniques for controlling and bounding the errors in quantities of interest are described in [5,25,38].

In [8,19,20,34] the authors introduce weight factors in the *a posteriori* error estimates to economically generate optimal meshes for the quantities of interest. Other applications of *a posteriori* error **estimates** in acoustic wave propagation and general solid and fluid mechanics are discussed in [13,14,26,28,33,35,36].

In addition to the above, there are several works, such as [43], exploiting *a posteriori* gradient reconstruction techniques. As detailed in [1,2,3,4] it is possible to define a gradient reconstruction operator which maps the finite element solution into an approximation of the gradient expected to be faster converging than the gradient of the approximate solution. Three pivotal conditions necessary for the gradient operator to yield a good approximation and an alternative option to higher order polynomial approximants are:

- *consistency:* the recovery operator should be able to reproduce exactly the true gradient when the dimension of the approximated problem tends to infinity;
- *localization:* the operator should not depend on global computations;
- *boundedness and linearity:* the recovery operator should be a linear bounded operator of its arguments.

Different approaches have been proposed in the literature. For example, in [6] the authors introduce a postprocessing operator constituted by an L^2 projection and a smoothing operation, which can recover the superconvergence property for any pth derivative of the solution for **finite-element** problems on unstructured but shape regular triangulations. We focused on the "superconvergent patch recovery" method [48], abbreviated as SPR, due to its high accuracy and computational efficiency for error-bounding applications [24]. The SPR technique for **finite-element** methods derives from the existence of the so-called Barlow points, see for example [7]. At such points, the gradient of the approximated solution possesses a convergence rate higher than elsewhere inside the element. Figure 1.1 provides an intuitive illustration of the reconstruction technique.

In [23,44,46,47] a mathematical analysis of the SPR technique is carried out for general quadrilateral finite elements. In recent years considerable efforts have been concentrated on enhancing the SPR method. For instance in [41] the authors propose a simultaneous interpolation of all the derivative components to improve efficiency. In [45] the SPR technique is applied directly on the solution in order to allow the use of unstructured meshes where the existence of the Barlow points is not always guaranteed [50]. In [16] the authors introduce an enhanced SPR technique able to recover at the same time both primal and dual solutions. Several works, such as [9,

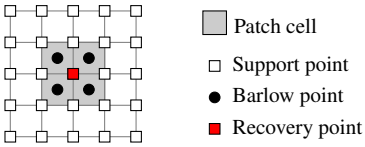

Fig. 1.1: Chosen the recovery point, the nearest Barlow points and the patch of cells that contains them are identified. A polynomial least square fit of the values of the gradient of the approximate solution at the Barlow points is then carried out.

37,42] have enhanced the standard SPR method adding constraints to satisfy internal equilibrium, compatibility, and boundary conditions.

The methods discussed above do not analyze the convergence **of functionals** of the solution, though. As highlighted in [8,15,29,32] and discussed in [15,29,30] the violation of the Galerkin orthogonality of the recovered solution results in lower accuracy and slower rates of convergence of the functionals.

In this work, we develop a novel gradient reconstruction technique that not only increases the accuracy but also preserves the convergence properties of functionals of the solution. To achieve the above, we enforce that the reconstructed gradient satisfies the Galerkin orthogonality condition. **This new technique requires to take into account the Riesz's representative w of the functional at hand, and to solve a dual problem which provides the finite-element projection w^h of the Riesz's representative. Overall, we are introducing another non-local problem which, in general, is not required by other standard approaches.**

The paper is structured into four sections: in Section 2 we present the problem statement together with a preliminary discussion on convergence. The above is followed in Section 3 by a brief formulation of the SPR approach and an *a priori* analysis of the convergence of the reconstructed solution. In Section 4 we motivate and describe our enhanced gradient reconstruction technique, abbreviated as SPR$^+$. In Section 5 we provide and discuss some numerical results obtained for different test cases.

2 Problem statement

Let us consider a generic elliptic problem with no reaction terms and mixed boundary conditions, defined in a bounded set Ω . The problem reads:

$$\textit{find } \boldsymbol{u}(\boldsymbol{x}) \textit{ such that:} \qquad \begin{cases} \nabla\cdot(\mathbb{C}\nabla\boldsymbol{u}) + \boldsymbol{f} = \boldsymbol{0} \quad \text{in } \Omega, \\ \\ \boldsymbol{u} = \bar{\boldsymbol{u}} \quad \text{on } \Gamma_D, \quad \mathbb{C}\nabla\boldsymbol{u}\cdot\boldsymbol{n} = \bar{\boldsymbol{t}} \quad \text{on } \Gamma_N, \end{cases} \tag{2.1}$$

where $\mathring{\Gamma}_D \cap \mathring{\Gamma}_N = \emptyset$ and $\overline{\Gamma_D \cup \Gamma_N} = \partial\Omega$. We assume the forcing term $\boldsymbol{f}$ and the boundary functions to be sufficiently regular. We also assume $\mathbb{C}(\boldsymbol{x})$ to be a bounded, positive-definite, symmetric tensor.

Let us denote by C the number of components of the unknown of the problem. We introduce the test functions space $\mathscr{V} := \{\boldsymbol{v} \in [\mathrm{H}^1(\Omega)]^C : \boldsymbol{\zeta}|_{\Gamma_D} = \boldsymbol{0}\}$ and

a new unknown field $\boldsymbol{z} := \boldsymbol{u} - \boldsymbol{R}_{\bar{\boldsymbol{u}}}$ where $\boldsymbol{R}_{\bar{\boldsymbol{u}}}$ is the lifting of the Dirichlet boundary data $\bar{\boldsymbol{u}}$. We then define the bilinear form $a : \mathscr{V} \times \mathscr{V} \to \mathbb{R}$, such that $a(\boldsymbol{\phi}, \boldsymbol{v}) := (\mathbb{C}\nabla\boldsymbol{\phi}, \nabla\boldsymbol{v})_\Omega$ for all $\boldsymbol{\phi}$ and $\boldsymbol{v} \in \mathscr{V}$, and the linear functional $F : \mathscr{V} \to \mathbb{R}$, such that $F(\boldsymbol{v}) := (\boldsymbol{f}, \boldsymbol{v})_\Omega + (\bar{\boldsymbol{t}}, \boldsymbol{v})_{\Gamma_N} - (\mathbb{C}\nabla\boldsymbol{R}_{\bar{\boldsymbol{u}}}, \nabla\boldsymbol{v})_\Omega$ for all $\boldsymbol{v} \in \mathscr{V}$. Thanks to the hypotheses made $a(\cdot,\cdot)$ is continuous and coercive and $F(\cdot)$ is bounded. With this notation at hand the variational problem can be formulated as:

$$\textit{find } \boldsymbol{z} \in \mathscr{V} \textit{ such that:} \qquad a(\boldsymbol{z}, \boldsymbol{v}) = F(\boldsymbol{v}), \qquad \forall \boldsymbol{v} \in \mathscr{V}. \tag{2.2}$$

Since all the hypotheses of the Lax-Milgram theorem are satisfied we conclude that the solution $\boldsymbol{z} \in \mathscr{V}$ of the variational problem (2.2) exists and is unique.

Let us consider a subdivision $\mathscr{T}_h := \bigcup_m K_m$ of the domain such that $\overline{\mathscr{T}_h} \equiv \overline{\Omega}$. We define the space $X_p^h := \{\boldsymbol{v}^h \in \left[\mathscr{C}^0(\mathscr{T}_h)\right]^C : \boldsymbol{v}^h|_{K_m} \in [\mathbb{P}_p(K_m)]^C,\ \forall K_m \in \mathscr{T}_h\}$ as the space of continuous piecewise polynomials of maximum degree $p \in \mathbb{N}$ on each subdomain K_m. Then we introduce the finite dimensional space $\mathscr{V}^h = \mathscr{V} \cap X_p^h$ and the finite element approximation of the solution $\boldsymbol{z}^h \in \mathscr{V}^h$. The Galerkin formulation of problem (2.2) reads:

$$\textit{find } \boldsymbol{z}^h \in \mathscr{V}^h \textit{ such that:} \qquad a(\boldsymbol{z}^h, \boldsymbol{v}^h) = F(\boldsymbol{v}^h), \qquad \forall \boldsymbol{v}^h \in \mathscr{V}^h.$$

Let us consider a linear and continuous functional $J : \mathscr{V} \to \mathbb{R}$ such that the quantity of interest that we want to compute is provided by the evaluation of J on the solution of the problem. Since the bilinear form $a(\cdot,\cdot)$ is continuous and coercive it defines an inner product on $\mathscr{V}$ and $(\mathscr{V}, a(\cdot,\cdot))$ is a Hilbert space whose norm is defined as $\|\boldsymbol{z}\|_{\mathscr{V}}^2 := a(\boldsymbol{z}, \boldsymbol{z})$. This implies that, thanks to a straightforward application of the Riesz's representation theorem, we are able to guarantee the existence of a unique solution $\boldsymbol{w} \in \mathscr{V}$ such that:

$$J(\boldsymbol{v}) = a(\boldsymbol{w}, \boldsymbol{v}), \qquad \forall \boldsymbol{v} \in \mathscr{V}, \tag{2.3}$$

and $\boldsymbol{w}$ is the Riesz's representative of the functional J in $(\mathscr{V}, a(\cdot,\cdot))$.

Hence considering a finite element space $\mathscr{W}^h := \mathscr{V} \cap X_q^h$ we define the discrete field $\boldsymbol{w}^h$ to be the solution of the Galerkin formulation of problem (2.3):

$$\textit{find } \boldsymbol{w}^h \in \mathscr{W}^h \textit{ such that:} \qquad J(\boldsymbol{v}^h) = a(\boldsymbol{w}^h, \boldsymbol{v}^h), \qquad \forall \boldsymbol{v}^h \in \mathscr{W}^h, \tag{2.4}$$

and $\boldsymbol{w}^h$ is the projection of the Riesz's representative $\boldsymbol{w}$ on the space $\mathscr{W}^h$.

We firstly observe that, if the solution is sufficiently regular, the convergence rate of the approximated gradient in the $\|\cdot\|_{\mathscr{V}}$-norm with respect to the characteristic mesh size h is equal to the polynomial degree denoted by p with constant $A \in \mathbb{R}^+$ independent of $\boldsymbol{z}$ and h:

$$\|\boldsymbol{z} - \boldsymbol{z}^h\|_{\mathscr{V}} \leq A h^p |\boldsymbol{z}|_{\mathrm{H}^{p+1}(\Omega)}. \tag{2.5}$$

Assuming the Riesz's representative to be sufficiently regular, *i.e.* at least $\boldsymbol{w} \in H^{p+1}(\Omega)$, through simple considerations we get the following *a priori* estimate for the error of the functional with constant $D \in \mathbb{R}^+$ independent of $\boldsymbol{z}$ and h:

$$|J(\boldsymbol{z}) - J(\boldsymbol{z}^h)| \leqslant D h^{2p} |\boldsymbol{w}|_{\mathrm{H}^{p+1}(\Omega)} |\boldsymbol{z}|_{\mathrm{H}^{p+1}(\Omega)}, \tag{2.6}$$

where the symmetry of the bilinear form $a(\cdot,\cdot)$ has been exploited together with the Galerkin orthogonality $a(\boldsymbol{z} - \boldsymbol{z}^h, \boldsymbol{w}^h) = 0$.

3 Superconvergent patch recovery technique (SPR)

It was experimentally observed in [7] that the approximated gradient converges with one order more than expected at the Barlow points. The SPR method consists in introducing an operator $\mathrm{G}_X : \mathscr{V}^h \to \mathscr{V}^h$ which defines a new finite element approximation of the exact gradient, that we denote by $\mathrm{G}_X[\boldsymbol{z}^h]$, which permits us to establish the following *a priori* estimate with constant $A \in \mathbb{R}^+$ independent of $\boldsymbol{z}$ and h:

$$\|\nabla \boldsymbol{z} - \mathrm{G}_X[\boldsymbol{z}^h]\|_{\mathrm{L}^2(\Omega)} \leq A h^{p+1} |\boldsymbol{z}|_{\mathrm{H}^{p+1}(\Omega)}. \tag{3.1}$$

A detailed analysis of the method is provided in [3].

At this point let us observe that there is no guarantee of the *a-orthogonality* of the error of the recovered gradient with respect to the space $\mathscr{V}^h$. To clarify this statement let us define the bilinear form $a_{\mathrm{SPR}} : \mathscr{V}^h \times \mathscr{V} \to \mathbb{R}$ as $a_{\mathrm{SPR}}(\boldsymbol{\phi}^h, \boldsymbol{v}) := (\mathbb{C}\mathrm{G}_X[\boldsymbol{\phi}^h], \nabla \boldsymbol{v})_\Omega$, for all $\boldsymbol{\phi}^h \in \mathscr{V}^h$ and for all $\boldsymbol{v} \in \mathscr{V}$. It is evident that the Galerkin orthogonality identity $a(\boldsymbol{z}, \boldsymbol{v}^h) = a(\boldsymbol{z}^h, \boldsymbol{v}^h)$ for all $\boldsymbol{v}^h \in \mathscr{V}^h$ is no longer generally satisfied. In fact, while $a(\boldsymbol{z}, \boldsymbol{v}^h) = F(\boldsymbol{v}^h)$, we have that there exists at least one $\boldsymbol{v}^h \in \mathscr{V}^h$ such that $a_{\mathrm{SPR}}(\boldsymbol{z}^h, \boldsymbol{v}^h) \neq F(\boldsymbol{v}^h)$.

Then defining the approximated evaluation of the functional J over the recovered gradient of the solution as $J_{\mathrm{SPR}}(\boldsymbol{z}^h) := a_{\mathrm{SPR}}(\boldsymbol{z}^h, \boldsymbol{w})$, we can prove the following error estimation with constant $D \in \mathbb{R}^+$ independent of $\boldsymbol{z}$, $\boldsymbol{w}$, and h:

$$|J(\boldsymbol{z}) - J_{\mathrm{SPR}}(\boldsymbol{z}^h)| \leqslant D h^{p+1} |\boldsymbol{w}|_{\mathrm{H}^1(\Omega)} |\boldsymbol{z}|_{\mathrm{H}^{p+1}(\Omega)}. \tag{3.2}$$

The last inequality (3.2) indicates that the accuracy and the convergence rate of the linear functional for the recovered solution is lower with respect to result (2.6).

4 SPR$^+$: a-orthogonality constrained SPR

We have enhanced the standard SPR approach by constraining the discrete least squares problem in a way such that the recovered gradient of the solution satisfies the *a-orthogonality* condition. Let us introduce the operator $\mathrm{G}_X^+ : \mathscr{V}^h \to \mathscr{V}^h$ which maps the solution to a reconstructed gradient $\mathrm{G}_X^+[\boldsymbol{z}^h]$. Then we define the bilinear form $a_{\mathrm{SPR}^+} : \mathscr{V}^h \times \mathscr{V} \to \mathbb{R}$ as $a_{\mathrm{SPR}^+}(\boldsymbol{\phi}^h, \boldsymbol{v}) := (\mathbb{C}\mathrm{G}_X^+[\boldsymbol{\phi}^h], \nabla \boldsymbol{v})_\Omega$, for all $\boldsymbol{\phi}^h \in \mathscr{V}^h$ and for all $\boldsymbol{v} \in \mathscr{V}$. To enforce the orthogonality constraint we employ Lagrange multipliers and we save the details of the implementation for Appendix A.3.

Let us now discuss the convergence of a linear functional $J : \mathscr{V} \to \mathbb{R}$ of the solution. We assume $\boldsymbol{w} \in \mathscr{V}$ to be the Riesz's representative of the functional and $\boldsymbol{w}^h \in \mathscr{W}^h := \mathscr{V} \cap X_q^h$ to be its finite element approximation. Here we define the space $X_q^h := \{\boldsymbol{v}^h \in \left[\mathscr{C}^0(\mathscr{T}_h)\right]^C : \boldsymbol{v}^h|_{K_m} \in [\mathbb{P}_q(K_m)]^C,\ \forall K_m \in \mathscr{T}_h\}$ as the space of continuous piecewise polynomials of maximum degree $q \in \mathbb{N}$ on each subdomain K_m. Then, defining $J_{\mathrm{SPR}^+}(\boldsymbol{z}^h) := a_{\mathrm{SPR}^+}(\boldsymbol{z}^h, \boldsymbol{w})$, **if the Riesz's representative is sufficiently regular, *i.e.* at least $\boldsymbol{w} \in H^{q+1}$,** it is easy to obtain the following error estimate with constant $D \in \mathbb{R}^+$ independent of $\boldsymbol{z}$, $\boldsymbol{w}$, and h:

$$|J(\boldsymbol{z}) - J_{\mathrm{SPR}^+}(\boldsymbol{z}^h)| \leqslant D h^{q+p+1} |\boldsymbol{w}|_{\mathrm{H}^{q+1}(\Omega)} |\boldsymbol{z}|_{\mathrm{H}^{p+1}(\Omega)}. \tag{4.1}$$

The previous result derives from a straightforward application of the constraint identity $a(\boldsymbol{z}, \boldsymbol{w}^h) - a_{\text{SPR}^+}(\boldsymbol{z}^h, \boldsymbol{w}^h) = 0$ and of inequality (2.5).

5 Numerical results

In this section, we present numerical results about errors measured for problems of the type (2.1) for three different test cases, one for each spatial dimension, with problem data summarized in Table A.1. For the sake of simplicity, all the tests have been run on equispaced structured meshes. We consider first linear finite element spaces and later, for the mono- and bi-dimensional cases, we analyze quadratic approximations. Besides, we investigate the convergence of the computed functional by varying the polynomial degree of the approximant of the dual solution $\boldsymbol{w}$ for a fixed $\boldsymbol{z}^h$.

Throughout this section we adopt the following notation:

$$\begin{aligned} &\boldsymbol{e}^h := \nabla z - \nabla z^h, \quad \boldsymbol{e}^h_{\text{SPR}} := \nabla z - \mathrm{G}_X\left[z^h\right], \quad \boldsymbol{e}^h_{\text{SPR}^+} := \nabla z - \mathrm{G}^+_X\left[z^h\right], \\ &eJ^h := J(z) - J(z^h), \quad eJ^h_{\text{SPR}} := J(z) - J_{\text{SPR}}(z^h), \quad eJ^h_{\text{SPR}^+} := J(z) - J_{\text{SPR}^+}(z^h). \end{aligned} \tag{5.1}$$

When the polynomial degree $q \in \mathbb{N}$ used for the computation of the finite element approximation of the Riesz's representative w^h (solution of problem (2.4)) is different to the degree p used to solve the problem, we use the notation $\text{SPR}^{+,q}$. We denote by $\boldsymbol{e}^h_*$ and eJ^h_* any of the errors listed in (5.1). Finally we consider linear functionals $J : \mathscr{V} \to \mathbb{R}$ of the solution having the following general structure:

$$J(v) = (\nabla v, \boldsymbol{\eta})_\Omega, \qquad \forall v \in \mathscr{V}, \tag{5.2}$$

where $\boldsymbol{\eta} \in [\mathrm{L}^2_\Omega]^d$ is a vectorial field defined case by case and d is the dimension of the problem.

5.1 Test cases

Tables 5.1a to 5.1c report the errors for each test case for piecewise linear approximants of the solution and of its dual. We observe that the convergence orders for the finite element method are in agreement with error estimate (2.5) while the SPR and SPR^+ techniques allow recovering one order of convergence for the gradient of the solution. In particular, the *a-orthogonality* constraint in the SPR^+ approach does not corrupt the recovered accuracy and convergence rates.

Convergence analysis of the linear functional of the solution is **summarized in** Tables 5.2a to 5.2c. We observe that the convergence rates for the FEM and SPR approaches are in agreement with error estimates (2.6) and (3.2), respectively, and that the SPR technique induces greater errors. On the contrary, it is interesting to observe that the SPR^+ method allows recovering the original accuracy and provides a convergence order equal to 4, which is one order more than predicted by inequality (4.1).

The results for piecewise quadratic polynomials (for the mono- and bi-dimensional cases alone due to the computational cost) are summarized in Tables 5.3a and 5.3b as

Table 5.1: Convergence results of solutions for the three test cases of mono-, bi- and tri-dimensional problems with piecewise linear finite elements $\mathcal{V}^h = \mathcal{V} \cap X_1^h$. The error in the gradient of the solution is reported for standard FEM, SPR and SPR$^+$.

(a) Convergence results of the solution of the monodimensional test case.

h/h_0	$\|\boldsymbol{e}^h\|_{\mathrm{L}^2(\Omega)}$	$\mathcal{O}$	$\|\boldsymbol{e}^h_{\mathrm{SPR}}\|_{\mathrm{L}^2(\Omega)}$	$\mathcal{O}$	$\|\boldsymbol{e}^h_{\mathrm{SPR}^+}\|_{\mathrm{L}^2(\Omega)}$	$\mathcal{O}$	$\|w - w^h\|_{\mathcal{V}}$	$\mathcal{O}$
1/1	$8.90 \cdot 10^{-2}$	–	$7.53 \cdot 10^{-3}$	–	$7.14 \cdot 10^{-3}$	–	$7.02 \cdot 10^{-2}$	–
1/2	$4.45 \cdot 10^{-2}$	1.00	$1.90 \cdot 10^{-3}$	1.98	$1.74 \cdot 10^{-3}$	2.04	$3.51 \cdot 10^{-2}$	1.00
1/4	$2.23 \cdot 10^{-2}$	1.00	$4.79 \cdot 10^{-4}$	1.99	$4.26 \cdot 10^{-4}$	2.03	$1.75 \cdot 10^{-2}$	1.00
1/8	$1.11 \cdot 10^{-2}$	1.00	$1.20 \cdot 10^{-4}$	2.00	$1.05 \cdot 10^{-4}$	2.02	$8.77 \cdot 10^{-3}$	1.00

(b) Convergence results of the solution of the bidimensional test case.

h/h_0	$\|\boldsymbol{e}^h\|_{\mathrm{L}^2(\Omega)}$	$\mathcal{O}$	$\|\boldsymbol{e}^h_{\mathrm{SPR}}\|_{\mathrm{L}^2(\Omega)}$	$\mathcal{O}$	$\|\boldsymbol{e}^h_{\mathrm{SPR}^+}\|_{\mathrm{L}^2(\Omega)}$	$\mathcal{O}$	$\|w - w^h\|_{\mathcal{V}}$	$\mathcal{O}$
1/1	$1.26 \cdot 10^{-1}$	–	$2.10 \cdot 10^{-2}$	–	$2.08 \cdot 10^{-2}$	–	$3.08 \cdot 10^{-1}$	–
1/2	$6.30 \cdot 10^{-2}$	1.00	$5.33 \cdot 10^{-3}$	1.98	$5.26 \cdot 10^{-3}$	1.98	$1.54 \cdot 10^{-1}$	1.00
1/4	$3.15 \cdot 10^{-2}$	1.00	$1.35 \cdot 10^{-3}$	1.99	$1.33 \cdot 10^{-3}$	1.99	$7.71 \cdot 10^{-2}$	1.00
1/8	$1.57 \cdot 10^{-2}$	1.00	$3.39 \cdot 10^{-4}$	1.99	$3.33 \cdot 10^{-4}$	1.99	$3.86 \cdot 10^{-2}$	1.00

(c) Convergence results of the solution of the tridimensional test case.

h/h_0	$\|\boldsymbol{e}^h\|_{\mathrm{L}^2(\Omega)}$	$\mathcal{O}$	$\|\boldsymbol{e}^h_{\mathrm{SPR}}\|_{\mathrm{L}^2(\Omega)}$	$\mathcal{O}$	$\|\boldsymbol{e}^h_{\mathrm{SPR}^+}\|_{\mathrm{L}^2(\Omega)}$	$\mathcal{O}$	$\|w - w^h\|_{\mathcal{V}}$	$\mathcal{O}$
1/1	$1.24 \cdot 10^{0}$	–	$1.84 \cdot 10^{0}$	–	$1.83 \cdot 10^{0}$	–	$1.38 \cdot 10^{1}$	–
1/2	$6.17 \cdot 10^{-1}$	1.00	$5.64 \cdot 10^{-1}$	1.70	$5.62 \cdot 10^{-1}$	1.71	$7.15 \cdot 10^{0}$	0.94
1/4	$3.08 \cdot 10^{-1}$	1.00	$1.51 \cdot 10^{-1}$	1.90	$1.50 \cdot 10^{-1}$	1.90	$3.61 \cdot 10^{0}$	0.99
1/8	$1.54 \cdot 10^{-1}$	1.00	$3.87 \cdot 10^{-2}$	1.96	$3.85 \cdot 10^{-2}$	1.96	$1.81 \cdot 10^{0}$	1.00

well as Tables 5.4a and 5.4b showcasing superconvergent gradients for both the SPR and SPR$^+$ methods while only superconvergent functionals for the SPR$^+$ method, consistently with what is observed for piecewise linear approximants.

5.2 Higher order polynomials for the approximation of the Riesz's representative

We have also investigated the convergence properties of the linear functional of the solution when adopting different degrees for the computation of the finite element approximation of the Riesz's representative $w^h \in \mathcal{W}^h := \mathcal{V} \cap X_q^h$.

We analyze the convergence properties of the SPR$^{+,q}$ technique for the bidimensional test case previously proposed (although similar results were observed for the other dimensions too) only for the resolution with piecewise linear polynomials. We increase the polynomial degree q adopted to compute w^h while we hold fixed the degree $p = 1$ used to solve the problem. The results are respectively described in Table 5.5 and show that the convergence order for the SPR$^{+,2}$ test is equal to 4, in agreement with the *a priori* error estimate (4.1). However, the solutions computed for the SPR$^{+,1}$ and SPR$^{+,3}$ problems provide convergence rates that are one order higher than predicted.

Table 5.2: Convergence results of the linear functional for the three test cases for the piecewise linear finite elements $\mathscr{V}^h = \mathscr{V} \cap X_1^h$ with piecewise linear approximant of the Riesz's representative.

(a) Convergence results of the linear functional of the monodimensional test case.

h/h_0	$\lvert eJ^h \rvert$	$\mathscr{O}$	$\lvert eJ^h_{\text{SPR}} \rvert$	$\mathscr{O}$	$\lvert eJ^h_{\text{SPR}^+} \rvert$	$\mathscr{O}$
1/1	$5.84 \cdot 10^{-3}$	–	$1.66 \cdot 10^{-2}$	–	$9.89 \cdot 10^{-5}$	–
1/2	$1.46 \cdot 10^{-3}$	2.00	$4.56 \cdot 10^{-3}$	1.87	$7.11 \cdot 10^{-6}$	3.80
1/4	$3.65 \cdot 10^{-4}$	2.00	$1.19 \cdot 10^{-3}$	1.94	$4.80 \cdot 10^{-7}$	3.89
1/8	$9.11 \cdot 10^{-5}$	2.00	$3.05 \cdot 10^{-4}$	1.97	$3.12 \cdot 10^{-8}$	3.94

(b) Convergence results of the linear functional of the bidimensional test case.

h/h_0	$\lvert eJ^h \rvert$	$\mathscr{O}$	$\lvert eJ^h_{\text{SPR}} \rvert$	$\mathscr{O}$	$\lvert eJ^h_{\text{SPR}^+} \rvert$	$\mathscr{O}$
1/1	$5.88 \cdot 10^{-3}$	–	$3.32 \cdot 10^{-2}$	–	$2.02 \cdot 10^{-4}$	–
1/2	$1.47 \cdot 10^{-3}$	2.00	$8.73 \cdot 10^{-3}$	1.93	$1.48 \cdot 10^{-5}$	3.77
1/4	$3.67 \cdot 10^{-4}$	2.00	$2.24 \cdot 10^{-3}$	1.97	$1.01 \cdot 10^{-6}$	3.87
1/8	$9.18 \cdot 10^{-5}$	2.00	$5.66 \cdot 10^{-4}$	1.98	$6.62 \cdot 10^{-8}$	3.93

(c) Convergence results of the linear functional of the tridimensional test case.

h/h_0	$\lvert eJ^h \rvert$	$\mathscr{O}$	$\lvert eJ^h_{\text{SPR}} \rvert$	$\mathscr{O}$	$\lvert eJ^h_{\text{SPR}^+} \rvert$	$\mathscr{O}$
1/1	$1.15 \cdot 10^{0}$	–	$5.26 \cdot 10^{0}$	–	$1.41 \cdot 10^{0}$	–
1/2	$2.71 \cdot 10^{-1}$	2.08	$1.87 \cdot 10^{0}$	1.49	$1.61 \cdot 10^{-1}$	3.13
1/4	$6.67 \cdot 10^{-2}$	2.02	$5.33 \cdot 10^{-1}$	1.81	$1.56 \cdot 10^{-2}$	3.37
1/8	$1.66 \cdot 10^{-2}$	2.01	$1.41 \cdot 10^{-1}$	1.91	$1.32 \cdot 10^{-3}$	3.57

Table 5.3: Convergence results of solutions for the test cases of monodimensional and bidimensional problems with piecewise quadratic finite elements $\mathscr{V}^h = \mathscr{V} \cap X_2^h$. The error in the gradient of the solution is reported for standard FEM, SPR and SPR$^+$.

(a) Convergence results of the solution of the monodimensional test case.

h/h_0	$\lVert \boldsymbol{e}^h \rVert_{\text{L}^2(\Omega)}$	$\mathscr{O}$	$\lVert \boldsymbol{e}^h_{\text{SPR}} \rVert_{\text{L}^2(\Omega)}$	$\mathscr{O}$	$\lVert \boldsymbol{e}^h_{\text{SPR}^+} \rVert_{\text{L}^2(\Omega)}$	$\mathscr{O}$	$\lVert w - w^h \rVert_{\mathscr{V}}$	$\mathscr{O}$
1/1	$1.13 \cdot 10^{-3}$	–	$6.54 \cdot 10^{-5}$	–	$6.22 \cdot 10^{-5}$	–	$6.31 \cdot 10^{-4}$	–
1/2	$2.82 \cdot 10^{-4}$	2.00	$8.19 \cdot 10^{-6}$	3.00	$7.80 \cdot 10^{-6}$	3.00	$1.58 \cdot 10^{-4}$	2.00
1/4	$7.05 \cdot 10^{-5}$	2.00	$1.02 \cdot 10^{-6}$	3.00	$9.76 \cdot 10^{-7}$	3.00	$3.95 \cdot 10^{-5}$	2.00
1/8	$1.76 \cdot 10^{-5}$	2.00	$1.28 \cdot 10^{-7}$	3.00	$1.22 \cdot 10^{-7}$	3.00	$9.86 \cdot 10^{-6}$	2.00

(b) Convergence results of the solution of the bidimensional test case.

h/h_0	$\lVert \boldsymbol{e}^h \rVert_{\text{L}^2(\Omega)}$	$\mathscr{O}$	$\lVert \boldsymbol{e}^h_{\text{SPR}} \rVert_{\text{L}^2(\Omega)}$	$\mathscr{O}$	$\lVert \boldsymbol{e}^h_{\text{SPR}^+} \rVert_{\text{L}^2(\Omega)}$	$\mathscr{O}$	$\lVert w - w^h \rVert_{\mathscr{V}}$	$\mathscr{O}$
1/1	$1.61 \cdot 10^{-3}$	–	$3.30 \cdot 10^{-4}$	–	$3.27 \cdot 10^{-4}$	–	$4.62 \cdot 10^{-3}$	–
1/2	$4.01 \cdot 10^{-4}$	2.01	$4.19 \cdot 10^{-5}$	2.97	$4.17 \cdot 10^{-5}$	2.97	$1.16 \cdot 10^{-3}$	2.00
1/4	$1.00 \cdot 10^{-4}$	2.00	$5.45 \cdot 10^{-6}$	2.94	$5.42 \cdot 10^{-6}$	2.94	$2.89 \cdot 10^{-4}$	2.00
1/8	$2.50 \cdot 10^{-5}$	2.00	$7.32 \cdot 10^{-7}$	2.90	$7.28 \cdot 10^{-7}$	2.90	$7.23 \cdot 10^{-5}$	2.00

Table 5.4: Convergence results of the linear functional for the mono- and bidimensional test cases for the piecewise quadratic finite elements $\mathscr{V}^h = \mathscr{V} \cap X_2^h$ with piecewise quadratic approximant of the Riesz's representative.

(a) Convergence results of the linear functional of the monodimensional test case.

h/h_0	$\lvert eJ^h \rvert$	$\mathscr{O}$	$\lvert eJ^h_{\mathrm{SPR}} \rvert$	$\mathscr{O}$	$\lvert eJ^h_{\mathrm{SPR}^+} \rvert$	$\mathscr{O}$
1/1	$5.87 \cdot 10^{-7}$	–	$1.01 \cdot 10^{-4}$	–	$1.41 \cdot 10^{-8}$	–
1/2	$3.67 \cdot 10^{-8}$	4.00	$1.23 \cdot 10^{-5}$	3.04	$4.22 \cdot 10^{-10}$	5.07
1/4	$2.29 \cdot 10^{-9}$	4.00	$1.51 \cdot 10^{-6}$	3.03	$1.28 \cdot 10^{-11}$	5.04
1/8	$1.37 \cdot 10^{-10}$	4.06	$1.87 \cdot 10^{-7}$	3.01	$3.00 \cdot 10^{-13}$	5.42

(b) Convergence results of the linear functional of the bidimensional test case.

h/h_0	$\lvert eJ^h \rvert$	$\mathscr{O}$	$\lvert eJ^h_{\mathrm{SPR}} \rvert$	$\mathscr{O}$	$\lvert eJ^h_{\mathrm{SPR}^+} \rvert$	$\mathscr{O}$
1/1	$1.01 \cdot 10^{-6}$	–	$3.52 \cdot 10^{-4}$	–	$2.21 \cdot 10^{-8}$	–
1/2	$6.31 \cdot 10^{-8}$	4.00	$4.28 \cdot 10^{-5}$	3.04	$9.06 \cdot 10^{-10}$	4.61
1/4	$3.94 \cdot 10^{-9}$	4.00	$5.26 \cdot 10^{-6}$	3.02	$3.12 \cdot 10^{-11}$	4.86
1/8	$2.39 \cdot 10^{-10}$	4.00	$6.52 \cdot 10^{-7}$	3.01	$4.39 \cdot 10^{-13}$	6.15

Table 5.5: Convergence results of the linear functional for the bidimensional test case when adopting different polynomial degrees for the computation of w^h while **keeping piecewise linear approximation** for the solution u^h.

h/h_0	$\lvert eJ^h_{\mathrm{SPR}^+,1} \rvert$	$\mathscr{O}$	$\lvert eJ^h_{\mathrm{SPR}^+,2} \rvert$	$\mathscr{O}$	$\lvert eJ^h_{\mathrm{SPR}^+,3} \rvert$	$\mathscr{O}$
1/1	$4.47 \cdot 10^{-2}$	–	$6.45 \cdot 10^{-4}$	–	$1.51 \cdot 10^{-6}$	–
1/2	$4.29 \cdot 10^{-3}$	3.38	$3.43 \cdot 10^{-5}$	4.23	$2.26 \cdot 10^{-8}$	6.06
1/4	$3.56 \cdot 10^{-4}$	3.59	$2.01 \cdot 10^{-6}$	4.10	$3.46 \cdot 10^{-10}$	6.03
1/8	$2.64 \cdot 10^{-5}$	3.75	$1.23 \cdot 10^{-7}$	4.03	$4.08 \cdot 10^{-12}$	6.40

5.3 Performance comparison

In Figure 5.1 we explore the error in the computed functional as against CPU time for the three different methods: FEM, SPR, and SPR$^+$. The results are related to the bidimensional test case, although similar results were observed for the other test cases. It is evident that, fixed the error under a reasonable accuracy, the SPR$^+$ technique is always preferable as the least computationally expensive approach.

Let us finally remark that the performance of the SPR$^+$ reconstruction algorithm can be further strengthened by localizing the reconstruction to subsets of the computational domain where the quantity of interest is to be computed (eg. around the crack tip in fracture mechanics to calculate the Stress Intensity Factors).

6 Conclusions

Linear functionals of the solution play a relevant role in engineering applications and goal-oriented adaptivity. We discovered that the non-optimal convergence properties induced by the SPR technique are related to the loss of the Galerkin orthogonality

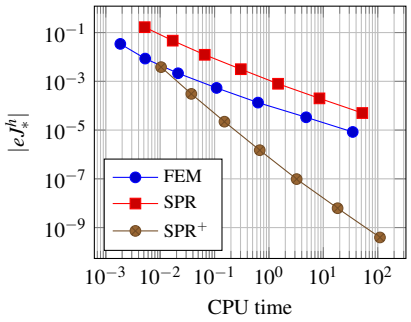

Fig. 5.1: Absolute value of the error of the linear functional over the CPU time when using piecewise linear polynomials for the computation of the solution.

condition which is naturally satisfied by the approximated solution computed with the finite element method.

The remedy that we have proposed in this work is provided by an enhanced variant of the SPR method, characterized by the addition of an orthogonality constraint to the discrete least squares problem that represents the SPR approach. Analyzing the numerical results obtained solving generic second-order elliptic problems in different dimensions we have observed that the constraint yields simultaneously a more accurate approximation of the gradient and linear functionals thereof.

A Appendix

A.1 Problem data for the numerical tests

In Table A.1 we summarize the problem data for the test cases of Section 5.

A.2 Implementation of the SPR method

In Section 3 we have introduced the reconstructed gradient $\mathrm{G}_X[\boldsymbol{z}^h](\boldsymbol{x})$ which is built on the Lagrangian tensorial basis functions $\{\Psi_l\}_{l=1}^L$ having maximum degree $p \in \mathbb{N}$ identical to the one used for the approximated solution $\boldsymbol{z}^h$ with nodal values $\{\zeta_l\}_{l=1}^L$:

$$\mathrm{G}_X[\boldsymbol{z}^h](\boldsymbol{x}) = \sum_{l=1}^{L} \zeta_l \Psi_l(\boldsymbol{x}). \tag{A.1}$$

The integer number L corresponds to the total number of degrees of freedom and is equal to $L = d \cdot C \cdot K$ where d is the dimension of the space, C represents the number of components of the unknown of the problem and K is the number of support points.

As illustrated in Figure 1.1, to each support point $\boldsymbol{x}_k$ it is associated at least one patch of cells $\mathscr{P}_k$ made of 2^d cells, such that $\boldsymbol{x}_k \in \mathscr{P}_k$. For each support point $\boldsymbol{x}_k$ there are $d \cdot C$ components of $\mathrm{G}_X[\boldsymbol{z}^h](\boldsymbol{x}_k)$ to reconstruct. Each m-th component of the reconstructed gradient, with $m \in \{1,\dots,d \cdot C\}$, is then approximated in a least squares sense by a complete polynomial centered in $\boldsymbol{x}_k$ of maximum degree p **coincident with** the degree used for the basis functions $\{\Psi_l\}_{l=1}^L$. Hence the polynomial approximation on the patch $\mathscr{P}_k$ writes:

$$\boldsymbol{a}_l \cdot \boldsymbol{p}(\boldsymbol{x}-\boldsymbol{x}_k), \qquad \forall \boldsymbol{x} \in \mathscr{P}_k,\ \forall l \in \mathbb{I}_k,\ k \in \{1,\dots,K\},$$

Table A.1: Problem parameters for the monodimensional (1D), bidimensional (2D) and tridimensional (3D) test cases.

(a) Description of the domain and its boundary decomposition and of the Dirichlet and Neumann boundary conditions for the three test cases. The Dirichlet boundary is defined as $\Gamma_D \equiv \partial\Omega \setminus (\Gamma_{N,1} \cup \Gamma_{N,2})$.

Test	Ω	$\Gamma_{N,1}$	$\Gamma_{N,2}$	$\bar{u}$	$\bar{t}_1$	$\bar{t}_2$
1D	$[-1,1]$	$\{1\}$	$\emptyset$	1	$-e\,\pi$	–
2D	$[-1,1]^2$	$\{1\}\times[-1,1]$	$[-1,1]\times\{1\}$	1	$-\pi\sin(\pi y)$	$-2\pi\sin(\pi x)$
3D	$[-1,1]^3$	$\emptyset$	$\emptyset$	0	–	–

(b) Exact expressions of the symmetric tensor $\mathbb{C}$, of the analytical solution u and of the exact Riesz's representative w of the functional J for the three test cases. The source term is computed as $f = -\nabla\cdot(\mathbb{C}\nabla u)$. The rank-2 tensor $\mathscr{I}$ represents the tridimensional identity tensor.

Test	$\mathbb{C}$	u	w
1D	e^x	$\sin(\pi x)+1$	$e^x(1-x^2)$
2D	$\begin{bmatrix} x^2 & xy \\ xy & y^2+1 \end{bmatrix}$	$\sin(\pi x)\sin(\pi y)+1$	$e^{2x}e^y(1-x^2)(1-y^2)$
3D	$\mathscr{I}$	$\sin(\pi x)\sin(\pi y)\sin(\pi z)$	$e^x e^{2y} e^{3z}(1-x^2)(1-y^2)(1-z^2)$

(c) Exact expressions of the field $\boldsymbol{\eta}$ adopted in identity (5.2) for the three test cases.

Test	$\boldsymbol{\eta}$
1D	$e^{2x}(1-2x-x^2)$
2D	$e^{2x}e^y\begin{bmatrix} 2x^2(1-x-x^2)(1-y^2)+xy(1-x^2)(1-2y-y^2) \\ 2xy(1-x-x^2)(1-y^2)+(y^2+1)(1-x^2)(1-2y-y^2) \end{bmatrix}$
3D	$\begin{bmatrix} e^x e^{2y} e^{3z}(1-2x-x^2)(1-y^2)(1-z^2) \\ 2e^x e^{2y} e^{3z}(1-x^2)(1-y-y^2)(1-z^2) \\ e^x e^{2y} e^{3z}(1-x^2)(1-y^2)(3-2z-3z^2) \end{bmatrix}$

where $\mathbb{I}_k$ is an interval of $d\cdot C$ indices related to the index k, that is $\mathbb{I}_k := \{d\cdot C\cdot(k-1)+1,\dots,d\cdot C\cdot k\}$, $\boldsymbol{a}_l \in \mathbb{R}^B$ represents the vector of the unknown coefficients and $\boldsymbol{p}(\boldsymbol{x}-\boldsymbol{x}_k) \in \mathbb{R}^B$ is the vector containing the polynomial basis functions. Then the nodal value ζ_l is set equal to the evaluation of the polynomial approximant at the recovery point:

$$\zeta_l = \boldsymbol{a}_l \cdot \boldsymbol{p}(\boldsymbol{0}). \tag{A.2}$$

The integer number B **coincides with** the number of Barlow points belonging to the current Patch $\mathscr{P}_k$, computed as:

$$B = \frac{\prod_{i=1}^{d}(p+i)}{d!}.$$

For any component $\left(\mathrm{G}_X[\boldsymbol{z}^h](\boldsymbol{x}_k)\right)_m$ the coefficients vector $\boldsymbol{a}_l$ is computed fitting the values of the gradient $\nabla\boldsymbol{z}^h$ at the B Barlow points $\{\boldsymbol{x}_b\}_{b=1}^B$ inside the patch $\mathscr{P}_k$ associated to $\boldsymbol{x}_k$, by resolution of a discrete least squares problem, which writes:

$$\min_{\boldsymbol{a}_l} \sum_{\boldsymbol{x}_b\in\mathscr{P}_k} \left|\boldsymbol{a}_l\cdot\boldsymbol{p}(\boldsymbol{x}_b-\boldsymbol{x}_k) - \left(\nabla\boldsymbol{z}^h(\boldsymbol{x}_b)\right)_m\right|^2, \tag{A.3}$$

where $m = (l-1)\bmod(d\cdot C)+1$. The operators div and mod represent respectively the integer division and the modulo operation.

The stationary point can be found by differentiation with respect to the minimization parameter $\boldsymbol{a}_l$. Setting the first-order derivative equal to zero we get the following linear algebraic system:

$$M_k \boldsymbol{a}_l = \boldsymbol{r}_l, \tag{A.4}$$

where the index k is related to the index l by the identity $k = (l-1)\,\mathrm{div}\,(d \cdot C) + 1$ and the matrix M_k and the right hand side $\boldsymbol{r}_l$ are defined as:

$$M_k := 2 \sum_{\boldsymbol{x}_b \in \mathscr{P}_k} \boldsymbol{p}(\boldsymbol{x}_b - \boldsymbol{x}_k)\, \boldsymbol{p}^{\mathrm{T}}(\boldsymbol{x}_b - \boldsymbol{x}_k), \qquad \boldsymbol{r}_l := 2 \sum_{\boldsymbol{x}_b \in \mathscr{P}_k} \Big(\nabla \boldsymbol{z}^h(\boldsymbol{x}_b)\Big)_m \boldsymbol{p}(\boldsymbol{x}_b - \boldsymbol{x}_k). \tag{A.5}$$

Hence for each support point $\boldsymbol{x}_k$ we solve $d \cdot C$ small linear problems (A.4) and we compute each nodal value ζ_l according to (A.2).

A.3 Implementation of the SPR$^+$ method

The constrained least squares problem that we want to solve has been discussed in Section 4 and derives from the SPR problem (A.6). We firstly rewrite the *a-orthogonality* condition as:

$$0 = a(\boldsymbol{z}, \boldsymbol{w}^h) - a_{\mathrm{SPR}^+}(\boldsymbol{z}^h, \boldsymbol{w}^h) = F(\boldsymbol{w}^h) - \sum_{r=1}^{L} \boldsymbol{a}_r \cdot \boldsymbol{p}(\boldsymbol{0})\, (\mathbb{C}\Psi_r, \nabla \boldsymbol{w}^h)_{\Omega_r},$$

where $\boldsymbol{z}^h \in \mathscr{V}^h$ and $\boldsymbol{w}^h \in \mathscr{W}^h$, as defined in Section 2. For any support point $\boldsymbol{x}_k$ and its associated patch $\mathscr{P}_k$, saying that we want to reconstruct the m-th component $\big(\mathrm{G}_X^+[\boldsymbol{z}^h](\boldsymbol{x}_k)\big)_m$, the constrained discrete least squares problem writes:

$$\begin{aligned} &\min_{\boldsymbol{a}_l} \sum_{\boldsymbol{x}_b \in \mathscr{P}_k} \left| \boldsymbol{a}_l \cdot \boldsymbol{p}(\boldsymbol{x}_b - \boldsymbol{x}_k) - \Big(\nabla \boldsymbol{z}^h(\boldsymbol{x}_b)\Big)_m \right|^2, \\ &\text{s.t.} \;\; F(\boldsymbol{w}^h) - \sum_{r=1}^{L} \boldsymbol{a}_r \cdot \boldsymbol{p}(\boldsymbol{0})\, (\mathbb{C}\Psi_r, \nabla \boldsymbol{w}^h)_{\Omega_r} = 0, \end{aligned} \tag{A.6}$$

where $\{\boldsymbol{x}_b\}_{b=1}^B$ are the Barlow points belonging to the patch $\mathscr{P}_k$. We adopt the Lagrange multiplier method, then let us define the multiplier $\lambda \in \mathbb{R}$ and the objective function of the problem $\mathscr{L}(\boldsymbol{a}_l; \lambda)$ as:

$$\mathscr{L}(\boldsymbol{a}_l; \lambda) := \sum_{\boldsymbol{x}_b \in \mathscr{P}_k} \left| \boldsymbol{a}_l \cdot \boldsymbol{p}(\boldsymbol{x}_b - \boldsymbol{x}_k) - \Big(\nabla \boldsymbol{z}^h(\boldsymbol{x}_b)\Big)_m \right|^2 + \lambda \left(F(\boldsymbol{w}^h) - \sum_{r=1}^{L} \boldsymbol{a}_r \cdot \boldsymbol{p}(\boldsymbol{0})\, (\mathbb{C}\Psi_r, \nabla \boldsymbol{w}^h)_{\Omega_r} \right). \tag{A.7}$$

We recall that $\{\boldsymbol{x}_b\}_{b=1}^B$ are the Barlow points belonging to the patch $\mathscr{P}_k$ associated to the recovery point $\boldsymbol{x}_k$ and the index k is related to the index l according to the rule $k = (l-1)\,\mathrm{div}\,(C \cdot d) + 1$. The index $m \in \{1, \ldots, d \cdot C\}$ refers to the component of the gradient that we want to reconstruct and is given by $m = (l-1)\,\mathrm{mod}\,(d \cdot C) + 1$.

The stationary point can be found by imposing the first order derivatives to be equal to zero. Differentiation by the coefficients vector $\boldsymbol{a}_l$ leads to:

$$M_k \boldsymbol{a}_l = \boldsymbol{r}_l + \lambda\, \boldsymbol{b}_l, \tag{A.8}$$

where the matrix M_k and the vector $\boldsymbol{r}_l$ have already been defined in (A.5). Then we have:

$$\boldsymbol{b}_l = \frac{\partial \left(\sum_r \boldsymbol{a}_r \cdot \boldsymbol{p}(\boldsymbol{0})\, (\mathbb{C}\Psi_r, \nabla \boldsymbol{w}^h)_{\Omega_r} \right)}{\partial \boldsymbol{a}_l} = (\mathbb{C}\Psi_l, \nabla \boldsymbol{w}^h)_{\Omega_l}\, \boldsymbol{p}(\boldsymbol{0}).$$

On the other hand differentiation by the Lagrange multiplier λ leads to the recovery of the constraint equation of problem (A.6), which writes:

$$F(\boldsymbol{w}^h) - \sum_{r=1}^{L} \boldsymbol{a}_r \cdot \boldsymbol{p}(\boldsymbol{0})\, (\mathbb{C}\Psi_r, \nabla \boldsymbol{w}^h)_{\Omega_r} = 0.$$

Substituting the explicit expression for $\boldsymbol{a}_l$ provided by result (A.8), we finally get the following solution for the Lagrange multiplier:

$$\lambda = \left(\sum_{l=1}^{L} \boldsymbol{b}_l \cdot M_k^{-1} \boldsymbol{b}_l \right)^{-1} \left[F(\boldsymbol{w}^h) - \sum_{l=1}^{L} \boldsymbol{b}_l \cdot M_k^{-1} \boldsymbol{r}_l \right].$$

References

1. Ainsworth M (2005) Robust a posteriori error estimation for nonconforming finite element approximation. SIAM Journal on Numerical Analysis 42(6):2320–2341
2. Ainsworth M, Babuska I (1999) Reliable and robust a posteriori error estimation for singularly perturbed reaction-diffusion problems. SIAM journal on numerical analysis 36(2):331–353
3. Ainsworth M, Oden JT (1993) A unified approach to a posteriori error estimation using element residual methods. Numerische Mathematik 65(1):23–50
4. Ainsworth M, Oden JT (2011) A posteriori error estimation in finite element analysis, vol 37. John Wiley & Sons
5. Ainsworth M, Rankin R (2012) Guaranteed computable bounds on quantities of interest in finite element computations. International Journal for Numerical Methods in Engineering 89(13):1605–1634
6. Bank R, Xu J, Zheng B (2007) Superconvergent derivative recovery for Lagrange triangular elements of degree p on unstructured grids. SIAM Journal on Numerical Analysis 45(5):2032–2046
7. Barlow J (1976) Optimal stress locations in finite element models. International Journal for Numerical Methods in Engineering 10(2):243–251
8. Becker R, Rannacher R (2001) An optimal control approach to a posteriori error estimation in finite element methods. Acta numerica 10:1–102
9. Blacker T, Belytschko T (1994) Superconvergent patch recovery with equilibrium and conjoint interpolant enhancements. International Journal for Numerical Methods in Engineering 37(3):517–536
10. Brenner S, Scott R (2007) The mathematical theory of finite element methods, vol 15. Springer Science & Business Media
11. Bürg M, Nazarov M (2015) Goal-oriented adaptive finite element methods for elliptic problems revisited. Journal of Computational and Applied Mathematics 287:125–147
12. Cao T, Kelly D (2003) Pointwise and local error estimates for the quantities of interest in two-dimensional elasticity. Computers & Mathematics with Applications 46(1):69–79
13. Cirak F, Ramm E (1998) A posteriori error estimation and adaptivity for linear elasticity using the reciprocal theorem. Computer Methods in Applied Mechanics and Engineering 156(1-4):351–362
14. Frolov M, Chistiakova O (2016) A new functional a posteriori error estimate for problems of bending of timoshenko beams. Lobachevskii Journal of Mathematics 37(5):534–540
15. Giles MB, Süli E (2002) Adjoint methods for pdes: a posteriori error analysis and postprocessing by duality. Acta Numerica 11:145–236
16. González-Estrada OA, Nadal E, Ródenas J, Kerfriden P, Bordas SPA, Fuenmayor F (2014) Mesh adaptivity driven by goal-oriented locally equilibrated superconvergent patch recovery. Computational Mechanics 53(5):957–976
17. Granzow BN, Shephard MS, Oberai AA (2017) Output-based error estimation and mesh adaptation for variational multiscale methods. Computer Methods in Applied Mechanics and Engineering 322:441–459
18. Grätsch T, Bathe KJ (2005) A posteriori error estimation techniques in practical finite element analysis. Computers & structures 83(4):235–265
19. Hartmann R, Houston P (2002) Adaptive discontinuous galerkin finite element methods for the compressible euler equations. Journal of Computational Physics 183(2):508–532
20. Hartmann R, Houston P (2006-01) Symmetric interior penalty dg methods for the compressible navier–stokes equations i: Method formulation. International Journal of Numerical Analysis and Modeling 3:1–20
21. Heintz P, Larsson F, Hansbo P, Runesson K (2004) Adaptive strategies and error control for computing material forces in fracture mechanics. International journal for numerical methods in engineering 60(7):1287–1299

22. Korotov S, Neittaanmäki P, Repin S (2003) A posteriori error estimation of goal-oriented quantities by the superconvergence patch recovery. Journal of Numerical Mathematics jnma 11(1):33–59
23. Křížek M, Neittaanmäki P (1987) On superconvergence techniques. Acta Applicandae Mathematica 9(3):175–198
24. Nadal E, De Almeida JPM, R denas JJ, Fuenmayor FJ, Gonz lez Estrada OA (2013) Application of a fully equilibrated superconvergent patch recovery scheme for error bounding. In: Adaptive Modeling and Simulation 2013 - Proceedings of the 6th International Conference on Adaptive Modeling and Simulation, ADMOS 2013, pp 503–514
25. Oden JT, Prudhomme S (2001) Goal-oriented error estimation and adaptivity for the finite element method. Computers & mathematics with applications 41(5-6):735–756
26. Oden JT, Prudhomme S (2002) Estimation of modeling error in computational mechanics. Journal of Computational Physics 182(2):496–515
27. Oden JT, Vemaganti KS (2000) Estimation of local modeling error and goal-oriented adaptive modeling of heterogeneous materials: I. error estimates and adaptive algorithms. Journal of Computational Physics 164(1):22–47
28. Oden JT, Prudhomme S, Demkowicz L (2005) A posteriori error estimation for acoustic wave propagation problems. Archives of Computational Methods in Engineering 12(4):343–389
29. Pierce NA, Giles MB (2000) Adjoint recovery of superconvergent functionals from pde approximations. SIAM review 42(2):247–264
30. Pierce NA, Giles MB (2004) Adjoint and defect error bounding and correction for functional estimates. Journal of Computational Physics 200(2):769–794
31. Quarteroni A (2010) Numerical models for differential problems, vol 2. Springer Science & Business Media
32. Rannacher R, Stuttmeier FT (1997) A feed-back approach to error control in finite element methods: application to linear elasticity. Comput Mech 19:434–446
33. Rannacher R (1998) A posteriori error estimation in least-squares stabilized finite element schemes. Computer methods in applied mechanics and engineering 166(1-2):99–114
34. Rannacher R (1999) Error control in finite element computations. In: Error control and adaptivity in scientific computing, Springer, pp 247–278
35. Rannacher R, Suttmeier FT (1999) A posteriori error estimation and mesh adaptation for finite element models in elasto-plasticity. Computer Methods in Applied Mechanics and Engineering 176(1-4):333–361
36. Repin S, Valdman J (2009) Functional a posteriori error estimates for incremental models in elasto-plasticity. Open Mathematics 7(3):506–519
37. Ródenas J, Tur M, Fuenmayor F, Vercher A (2007) Improvement of the superconvergent patch recovery technique by the use of constraint equations: the spr-c technique. International Journal for Numerical Methods in Engineering 70(6):705–727
38. Rozza G, Huynh DBP, Patera AT (2008) Reduced basis approximation and a posteriori error estimation for affinely parametrized elliptic coercive partial differential equations. Archives of Computational Methods in Engineering 15(3):229
39. Venditti DA, Darmofal DL (2000) Adjoint error estimation and grid adaptation for functional outputs: Application to quasi-one-dimensional flow. Journal of Computational Physics 164(1):204–227
40. Verfürth R (1996) A review of a posteriori error estimation and adaptive mesh-refinement techniques. John Wiley & Sons Inc
41. Wiberg NE, Abdulwahab F (1993) Patch recovery based on superconvergent derivatives and equilibrium. International Journal for Numerical Methods in Engineering 36(16):2703–2724
42. Wiberg NE, Abdulwahab F, Ziukas S (1994) Enhanced superconvergent patch recovery incorporating equilibrium and boundary conditions. International Journal for Numerical Methods in Engineering 37(20):3417–3440
43. Xuan Z, Yang D, Peng J (2008) An efficient method for computing local quantities of interest in elasticity based on finite element error estimation. Archive of Applied Mechanics 78(7):517–529
44. Zhang Z (2000) Ultraconvergence of the patch recovery technique ii. Mathematics of Computation of the American Mathematical Society 69(229):141–158
45. Zhang Z, Naga A (2005) A new finite element gradient recovery method: superconvergence property. SIAM Journal on Scientific Computing 26(4):1192–1213
46. Zhang Z, Victory Jr HD (1996) Mathematical analysis of zienkiewicz-zhu's derivative patch recovery technique. Numerical Methods for Partial Differential Equations 12(4):507–524
47. Zhu Q, Zhao Q (2003) Spr technique and finite element correction. Numerische Mathematik 96(1):185–196

48. Zienkiewicz OC, Zhu JZ (1992) The superconvergent patch recovery and a posteriori error estimates. part 1: The recovery technique. International Journal for Numerical Methods in Engineering 33(7):1331–1364
49. Zienkiewicz OC, Taylor RL, Zhu J (1977) The finite element method, vol 3. McGraw-hill London
50. Zienkiewicz OC, Taylor RL, Zhu J (2013) The Finite Element Method: Its Basis and Fundamentals. Elsevier, Incorporated